Oscillation suppression in indirectly coupled limit cycle oscillators

Neeraj Kumar Kamal, Pooja Rani Sharma, and Manish Dev Shrimali
Department of Physics, Central University of Rajasthan, Ajmer 305 817, India
(Received 6 May 2015; revised manuscript received 28 July 2015; published 31 August 2015)

We study the phenomena of oscillation quenching in a system of limit cycle oscillators which are coupled indirectly via a dynamic environment. The dynamics of the environment is assumed to decay exponentially with some decay parameter. We show that for appropriate coupling strength, the decay parameter of the environment plays a crucial role in the emergent dynamics such as amplitude death (AD) and oscillation death (OD). The critical curves for the regions of oscillation quenching as a function of coupling strength and decay parameter of the environment are obtained analytically using linear stability analysis and are found to be consistent with the numerics.

DOI: 10.1103/PhysRevE.92.022928 PACS number(s): 05.45.Xt

I. INTRODUCTION

Understanding of coupled oscillators provides an elegant way to realize a variety of complex dynamical behaviors, arising spontaneously in real-life systems [1–3]. Recently, the fascinating phenomenon of oscillation quenching, i.e., amplitude death (AD) [4] and oscillation death (OD) [5], has been extensively studied due to its applications in various fields including physics, biology, chemistry, and engineering. Amplitude death corresponds to a situation in which the oscillations of coupled oscillators are suppressed in such a way that they stabilize to the same stable steady state which was otherwise unstable. First observed by Rayleigh [1] in nineteenth century, this phenomenon has been studied with different coupling schemes to understand its properties and causes of manifestation [4] in diverse areas ranging from oceanography [6] and chemical engineering [7] to lasers [8] and neuronal systems [9].

On the other hand, oscillation death refers to stable inhomogeneous steady states (IHSS), where oscillators occupy different steady states which are created by the coupling. The key ingredient for this type of emergent dynamics is the breaking of the inherent symmetry of the system [5]. Thus, in contrast to AD, OD is a much more complex phenomenon, since it stimulates inhomogeneity in a rather homogeneous system of oscillators. Occurrence of oscillation death (OD) is quite common in many natural systems such as chemical oscillators [10], chemical droplets [11], chemical reactors [12], thermokinetic oscillators [13], and electronic circuits [14]. Moreover, eminent significance of OD can be clearly realized in the case of biological systems including neural networks [15], genetic oscillators [16], calcium oscillators [17], and stem cell differentiation [18].

Since AD and OD both represent the state of suppressed oscillations, they therefore have been considered as the same phenomena for many years. It is only in the recent findings of Koseska *et al.* [5] where the distinction between these two structurally different states has been pointed out. In this work, it is articulated that AD and OD are two entirely different phenomena in their nascency as well as in their properties. Over the past few years, this peculiar phenomenon of OD has been profoundly explored and shown to subsist under various coupling schemes, for example, dynamic and conjugate coupling [19], time-delay coupling [20], mean-field coupling [21–25], repulsive coupling [26], direct-indirect coupling [27,28], etc.

The recent surge in studies related to the collective behavior of indirectly coupled oscillators [29–36] is motivated by the fact that elements in some realistic systems influence each other indirectly through a common medium. For instance, chemical oscillations of catalyst loaded reactants in a medium exchange chemicals with the surrounding medium [37]. Genetic oscillators also communicate to each other by diffusing chemicals between cells and the extracellular medium [38]. Similarly, an ensemble of cold atoms also interact through a coherent electromagnetic field [39]. The framework of indirect coupling also provides a better understanding of the functioning and operating mechanism of the biological systems such as bacteria [40] and yeast cells [41] that communicate through a common environment. In addition, emergence of robust rhythms in biological organisms such as central pattern generators, cardiac pacemakers, and circadian clocks are also well explained by indirectly coupled oscillators. Moreover, for the case of neuronal oscillators, this kind of coupling has particular meaning where concentrations of neurotransmitters released by each cell stimulate collective rhythms in a population of circadian oscillators [42]. In order to capture the essential features of such systems, Resmi *et al.* proposed a model of indirectly coupled oscillators. They have shown that the phenomena of synchronization and amplitude death [34–36] emerge due to the interplay of direct and indirect coupling in such systems. Later, the occurrence of OD was also studied by Ghosh *et al.* [28] under the same coupling scheme.

The study about the collective dynamics of a system of oscillators, coupled only via external environment, is a less explored area and only a few studies are devoted to this subject. For example, in an ensemble of indirectly coupled chaotic oscillators with no direct coupling, the phenomena of synchronization and quorum-sensing behavior has been investigated [43]. Moreover, dynamical quorum sensing was also observed for an ensemble of oscillators which were coupled diffusively through an external medium [44]. However, the phenomena of oscillation quenching has not been explored for the system of oscillators where communication among them is through a common medium. In this work, we explore the possibility of the existence of AD and OD in a system of indirectly coupled oscillators where direct interaction among them is absent. We identify various quenched oscillation states, namely, amplitude death (AD), homogeneous steady states (HSS), and inhomogeneous steady states (IHSS). Using detailed bifurcation analysis, we also

explore the transition from one quenched oscillation state to another.

The outline of the paper is as follows. In Sec. II, we discuss the model and find different nontrivial steady states possible for the system. In Sec. III, we first present the numerical phase diagram in the parameter plane showing different dynamical regimes possible for the system and then corroborate the numerical results with analytical results, obtained from linear stability analysis and bifurcation diagram obtained from the package XPPAUT [45]. Finally, in Sec. IV we summarize the results.

II. MODEL

To demonstrate the effect of indirect coupling on limit cycle oscillators, we consider the Stuart-Landau (SL) oscillator as a basic unit described by the equation

$$\dot{z} = f(z) = (1 + i\omega - |z|^2)z, \tag{1}$$

where $z = re^{i\theta} = x + iy$ is the state variable, with real part $\mathrm{Re}(z) = x$ and imaginary part $\mathrm{Im}(z) = y$. This system exhibits self-sustained limit cycle oscillations with radius $r = 1$ and frequency ω [46,47].

The system of 2 ($N > 1$) SL oscillators, coupled through a common environment, is given as

$$\begin{aligned} \dot{z}_1 &= (1 + i\omega_1 - |z_1|^2)z_1 + \epsilon(s - x_1), \\ \dot{z}_2 &= (1 + i\omega_2 - |z_2|^2)z_2 + \epsilon(s - x_2), \\ \dot{s} &= -\gamma s - \epsilon\left(\frac{x_1 + x_2}{2}\right). \end{aligned} \tag{2}$$

Here, the state variable s corresponds to the external environment and ϵ ($\epsilon > 0$) is the coupling strength. It is the measure of particle species that can freely diffuse in the environment and allows oscillators to communicate with each other. The environment has its own dynamics and in the absence of coupling it is decaying with the decay rate γ. This model of indirectly coupled oscillators is able to capture the gist of many chemical and biological systems. In these systems, through diffusion of common species, elements influence the environment and also get influenced by the environment. Here, the dynamical equations of the two oscillators are invariant under the permutation of indices. Nevertheless, the *continuous rotational symmetry* present in the single SL oscillator is broken by the coupling term and results in different nontrivial steady states. This work emphasizes the stability of these newly created *homogeneous* and *inhomogeneous* steady states due to interaction. Without any loss of generality, we set the internal frequency of each oscillator at $\omega_1 = \omega_2 = \omega = 2$ initially.

In order to study the behavior of homogeneous and inhomogeneous fixed points, we introduce the following linear coordinate transformation:

$$z_s = \tfrac{1}{2}(z_1 + z_2); \qquad z_a = \tfrac{1}{2}(z_1 - z_2); \tag{3}$$

which are symmetric and antisymmetric variables and correspond to *symmetric* ($z_a = 0$) and *antisymmetric* ($z_s = 0$) manifolds respectively. In this coordinate system the dynamical equations transform to

$$\begin{aligned} \dot{z_s} &= \tfrac{1}{2}[f(z_s + z_a) + f(z_s - z_a)] - \epsilon[s - \mathrm{Re}(z_s)], \\ \dot{z_a} &= \tfrac{1}{2}[f(z_s + z_a) - f(z_s - z_a)] - \epsilon\mathrm{Re}(z_a), \\ \dot{s} &= -\gamma s - \epsilon\mathrm{Re}(z_s). \end{aligned} \tag{4}$$

Thus, the dynamical equations from Eqs. (4) can be written as [20]

$$\begin{aligned} \dot{z_s} &= \left(1 + i\omega - |z|_s^2\right)z_s - \epsilon[s - \mathrm{Re}(z_s)], \\ \dot{s} &= -\gamma s - \epsilon\mathrm{Re}(z_s), \\ \dot{z_a} &= 0 \end{aligned} \tag{5}$$

for the *symmetric subspace*, $Z_s = \{(z_s,s,z_a)|z_a \equiv 0\}$, and

$$\begin{aligned} \dot{z_s} &= 0, \\ \dot{s} &= 0, \\ \dot{z_a} &= \left(1 + i\omega - |z|_a^2\right)z_a - \epsilon\mathrm{Re}(z_a) \end{aligned} \tag{6}$$

for the *antisymmetric subspace*, $Z_a = \{(z_s,s,z_a)|z_s \equiv 0, s \equiv 0\}$.

Clearly, apart from the trivial homogeneous steady state, $(z_1,z_2,s) = (0,0,0)$, Eqs. (5) and (6) also allow the appearance of nontrivial steady states in *symmetric* and *antisymmetric* subspaces for the above system. Thus, from the equations obtained above we can calculate the fixed points of the coupled system and can also perform their stability analysis.

Note that the antisymmetric subspace allows only *inhomogeneous* solutions. Two different branches b_1 and b_2 of steady-states solutions, represented as $(z_s,s,z_a) = (0,0,\pm z^{ih}_{b_1})$ and $(z_s,s,z_a) = (0,0,\pm z^{ih}_{b_2})$, emerge from the trivial steady state $(z_1,z_2,s) = (0,0,0)$ and are given by

$$\begin{aligned} x^{ih}_{b_1,b_2} &= y^{ih}_{b_1,b_2}\left(\frac{\mp\epsilon + \sqrt{\epsilon^2 - 4\omega^2}}{2\omega}\right), \\ y^{ih}_{b_1,b_2} &= \sqrt{\frac{\epsilon - 2\omega^2 \pm \sqrt{\epsilon^2 - 4\omega^2}}{2\epsilon}}; \end{aligned} \tag{7}$$

where $z^{ih}_{b_1,b_2} = x^{ih}_{b_1,b_2} + iy^{ih}_{b_1,b_2}$. Also note that solution of the system will be of the form $x_1 = -x_2$ and $y_1 = -y_2$ and therefore, if the system stabilizes to any of the solution branches b_1 or b_2, it is called *oscillation death*. Moreover, the superscript ih denotes the inhomogeneous steady state.

For the symmetric subspace, by definition, only *homogeneous* steady states can be found. The HSS of the system for symmetric subspace also emerges from trivial steady state, $(z_1,z_2,s) = (0,0,0)$. The two solution branches of homogeneous steady states are represented as $(z_s,s,z_a) = (z^h_{b_1},s_{b_1},0)$ and $(z_s,s,z_a) = (z^h_{b_2},s_{b_2},0)$ and given by

$$\begin{aligned} x^h_{b_1,b_2} &= y^h_{b_1,b_2}\left(\frac{\mp\epsilon(\epsilon + \gamma) + \sqrt{\epsilon^2(\epsilon + \gamma)^2 - 4\omega^2\gamma^2}}{2\omega\gamma}\right), \\ y^h_{b_1,b_2} &= \sqrt{\frac{\epsilon(\epsilon + \gamma) - 2\omega^2\gamma \pm \sqrt{\epsilon^2(\epsilon + \gamma)^2 - 4\omega^2\gamma^2}}{2\epsilon\gamma}}, \\ s_{b_1,b2} &= -x^h_{b_1,b_2}\frac{\epsilon}{\gamma}; \end{aligned} \tag{8}$$

where $z^h_{b_1,b_2} = x^h_{b_1,b_2} + iy^h_{b_1,b_2}$. Here, the superscript h stands for homogeneous steady states. If the system stabilizes to any of the solution branch, b_1 and b_2, it is called *amplitude death* as in this case both the solutions are of the form, $x_1 = x_2 \quad \text{and} \quad y_1 = y_2$.

The rotational symmetry of the uncoupled system [given by Eq. (1) for $\epsilon = 0$] is broken by the coupling term leading to the appearance of HSS ($z_1 = z_2$) and IHSS ($z_1 = -z_2$) solutions of Eq. (2) [5].

III. RESULTS

Regions of different dynamical states of the system of two indirectly coupled oscillators in the parameter plane of coupling strength, ϵ, and decay rate of linear system, γ, are calculated numerically and shown in Fig. 1. For each set of parameters ϵ and γ we have chosen 10^2 initial conditions for each oscillator as well as for the environment from a uniform random distribution in the range $(-1,1)$. In Fig. 1, AD refers to stabilization of the system to the trivial fixed point, namely the *origin,* while HSS and IHSS represent homogenous steady states and inhomogenous steady states, respectively. Moreover, the black curves are the analytical results, obtained from the eigenvalue analysis. The stability of steady states is determined by the eigenvalues of the Jacobian matrix calculated at the fixed points. If the real part of the largest eigenvalue of this matrix is negative, then the corresponding steady state is stable; otherwise it is unstable. Additionally, we also define the unstable dimension for the system, which is the number of strictly positive eigenvalues of the Jacobian matrix at the corresponding fixed point. Clearly, the unstable dimension will be zero for the stable fixed point in the parameter plane.

We first consider the stability of origin in the parameter plane (ϵ, γ). For this state, the characteristic equation in the symmetric subspace is given as

$$\lambda^3 + a_2\lambda + a_1\lambda + a_0 = 0, \tag{9}$$

with $a_2 = \gamma - 2 + \epsilon$, $a_1 = 1 + \omega^2 - 2\gamma + \epsilon^2 + \gamma\epsilon - \epsilon$ and $a_0 = \gamma(1+\omega^2) - \epsilon^2 - \epsilon\gamma$ and in the antisymmetric subspace

$$\lambda^2 + \lambda(\epsilon - 2) + (1 + \omega^2 - \epsilon) = 0. \tag{10}$$

Now, the solutions of these two equations decide the stability of origin. At $\epsilon = 2$ the real part of the two eigenvalues of antisymmetric subspace crosses zero. Also, the remaining three eigenvalues corresponding to symmetric subspace are found to be negative, which leads to the occurrence of Hopf bifurcation.

Now, the HSS solutions are born at $\gamma = \gamma_c$ where

$$\gamma_c = \frac{\epsilon^2}{1 - \epsilon + \omega^2}. \tag{11}$$

In the parameter plane of ϵ and γ, the curves $\epsilon = 2$ and $\gamma = \gamma_c$ meet at $\gamma = \frac{4}{\omega^2 - 1} = 1.333$. So, for $\gamma > 1.333$ the origin is stabilized via Hopf bifurcation. Using the Routh-Hurwitz criterion of roots for polynomial equation, we find that for $\gamma > \gamma_c$ roots of Eq. (9) cross the y axis and become positive, resulting in the destabilization of the AD solution. Thus, the region of stability of origin lies within the boundary of two curves, namely, $\epsilon = 2$ and $\gamma = \gamma_c$. The statements made above are well corroborated with the phase diagram (Fig. 1) and the bifurcation diagram [Fig. 2(a)]. A typical time series of

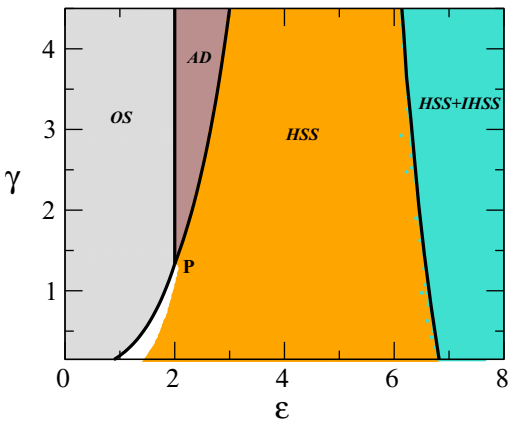

FIG. 1. (Color online) Diagram showing different phases of coupled system in the parameter plane of ϵ and γ. The different colors represent different dynamical regimes. White color corresponds to a state where oscillatory solutions coexist with HSS solutions. Other dynamical regimes are marked as OS, AD, HSS, and HSS + IHSS (for details, please see text). The black curves separating different dynamical regimes are obtained analytically using linear stability analysis at $\omega = 2$.

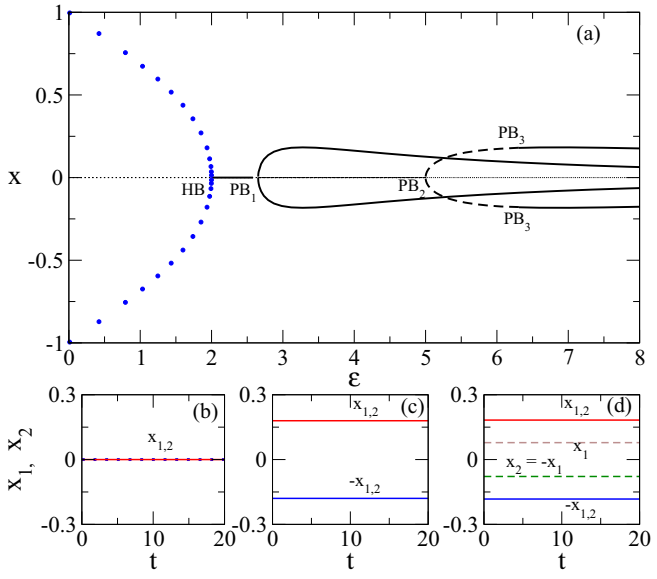

FIG. 2. (Color online) (a) Bifurcation diagram (using XPPAUT) of two coupled SL oscillators is plotted as a function of coupling strength, ϵ. Solid and dashed lines denote stable and unstable steady states, respectively, while filled blue (gray) circles represent stable periodic solutions. The bifurcation points such as Hopf bifurcation (HB) and pitchfork bifurcation (PB) are marked. Time series of state variable x for the two oscillators at (b) $\epsilon = 2.5$ showing AD, i.e., $x_{1,2} = 0$; (c) $\epsilon = 3.5$ showing HSS solutions where $x_1 = x_2$; and (d) at $\epsilon = 7$ representing both HSS (shown by red and blue [gray] lines) and IHSS solutions (dashed lines), where $x_1 = -x_2$. Here, $\gamma = 3 > \gamma_c$ and $\omega = 2$.

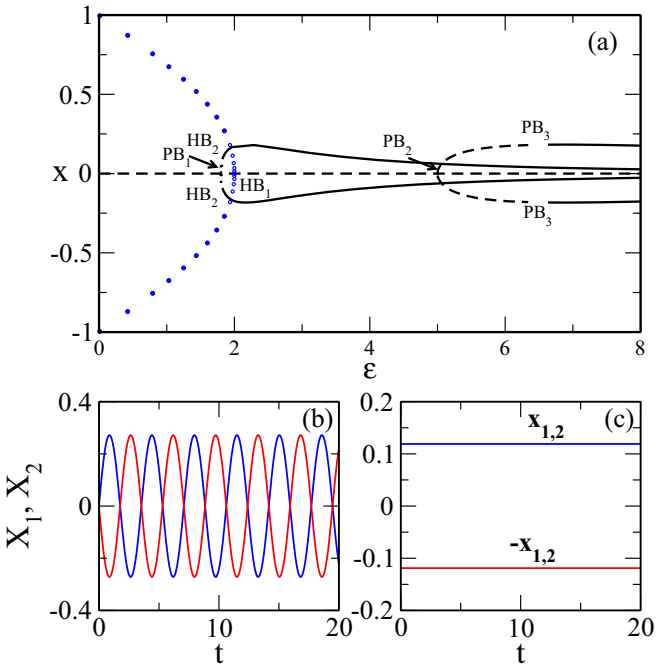

FIG. 3. (Color online) (a) Bifurcation diagram (using XPPAUT) of the two SL oscillators is plotted as a function of coupling strength, ϵ. Solid and dashed lines denote stable and unstable steady states, respectively, while filled and open blue (gray) circles stand for stable and unstable periodic solutions, respectively. The bifurcation points, namely Hopf bifurcation (HB) and pitchfork bifurcation (PB), are marked. Time series of state variable x of the two oscillator for $\epsilon = 1.85$ for two different initial conditions showing (b) antiphase periodic solutions and (c) HSS solutions. The other parameters $\gamma = 1 < \gamma_c$ and $\omega = 2$.

x variable of the two oscillators for this dynamical regime is shown in Fig. 2(b).

The HSS solutions born at $\gamma = \gamma_c$ are stabilized by pitchfork bifurcation as marked by PB_1 in Fig. 2(a) for $\gamma = 3 > 1.333$. However, at $\gamma = 1.333$ both pitchfork and Hopf bifurcation points merge, which results in the destabilization of both periodic as well as the HSS solutions in the system. The merging of pitchfork bifurcation point and Hopf bifurcation point is also clearly visible in the phase diagram (Fig. 1) by the point marked by P. In this case, both HSS and oscillatory solutions coexist with each other. A representative time series of x variable of both oscillators is shown in Figs. 3(b) and 3(c). Here we have used different initial conditions for a particular parameter values $\epsilon = 1.85$ and $\gamma = 1$. Note that the oscillatory solutions are in antiphase and can be seen in Fig. 3(b), which is quite different from the cases which have been reported earlier [12,23]. To check the stability of the HSS solution, we consider the characteristic equation corresponding to HSS solutions in both symmetric and antisymmetric subspaces. In symmetric subspace it is given as

$$\lambda^3 + b_2\lambda^2 + b_1\lambda + b_0 = 0, \tag{12}$$

where $b_2 = 4r^2 + \epsilon - 2 + k$, $b_1 = 1 + \omega^2 + 3r^4 - 4r^2 + \epsilon(r^2 + 2y^2 - 1) + \gamma(4r^2 + \epsilon - 2)$, and $b_0 = \gamma(1 + \omega^2 + 3r^4 - 4r^2) + \epsilon(r^2 + 2y^2 - 1)(\gamma + \epsilon)$. The characteristic equation of HSS in antisymmetric subspace is given by

$$\lambda^2 + c_1\lambda + c_0 = 0, \tag{13}$$

where $c_1 = 4r^2 + \epsilon - 2$ and $c_0 = 1 + \omega^2 + 3r^4 - 4r^2 + \epsilon(r^2 + 2y^2 - 1)$. In Eqs. (12) and (13) $r^2 = x^2 + y^2$ with the value of x and y as given in Eq. (8). Here, we have also used Routh-Hurwitz criterion and observed that for $\gamma < 1.333$ the eigenvalues of symmetric subspace are negative and only one eigenvalue of the antisymmetric subspace is positive. However, this positive eigenvalue become negative at the critical value of γ given as

$$\gamma = \frac{4\epsilon^2(\epsilon + 2)}{4(1 + \omega^2) - \epsilon(3\epsilon + 4)}. \tag{14}$$

Thus, the region of stability for HSS lies on the right side of the curve given by Eq. (11) for $\gamma > 1.333$ and Eq. (14) for $\gamma < 1.333$. The phase diagram portrayed in Fig. 1 and bifurcation diagrams displayed in Figs. 2(a) and 3(a) also validate the statements made above. The time series of x variable of the two oscillators is plotted for $\gamma = 3$ and $\epsilon = 3.5$ in Fig. 2(c), which shows the two stable HSS solutions for two different initial conditions.

Now, the IHSS solutions are born via pitchfork bifurcation at $\epsilon = 1 + \omega^2$ as marked by PB_2 in Figs. 2(a) and 3(a). Behavior of this state is analyzed by considering the characteristic equations for these points. It turns out that the characteristic equation obtained for this state in symmetric and antisymmetric subspaces is same as that of the HSS solutions given by Eqs. (12) and (13). However, the difference is of IHSS value, as given by Eq. (7). Using the Routh-Houritz criterion, for the two equations we find that all eigenvalues are negative except one in symmetric subspace, thus reducing the unstable dimension of the system to one. Since the analytical expression for the curve in ϵ and γ parameter space is complicated, we take some representative values of ϵ and calculate the values of γ numerically, where all the eigenvalues are negative. These points are plotted in the phase diagram (Fig. 1) and match with the stability boundary of IHSS. It turns out that these IHSS solutions are stabilized by another pitchfork bifurcation (PB_3) as articulated in Figs. 2(a) and 3(a). Here, the IHSS solutions coexist with HSS solutions, which can be seen in the time series of state variable x of both oscillators in Fig. 2(d) for $\epsilon = 7$ and $\gamma = 3$. Here, depending on the initial conditions, oscillations of two oscillators are quenched in such a way that the state variable can be either in symmetric, i.e., $x_1 = x_2, y_1 = y_2$, or in antisymmetric, i.e., $x_1 = -x_2, y_1 = -y_2$, state.

Now we will discuss the other important aspect, which is the stability of the HSS solutions in the case of *parameter mismatch*. We have introduced the mismatch parameter Δ in Eq. (2) with $\Delta = \omega_1 - \omega_2$. Clearly, the case $\Delta = 0$ represents identical systems. For $\Delta \neq 0$, we numerically compute the phase diagram to understand the emergent behavior of the system due to mismatch. Figure 4(a) shows the phase diagram for the coupled system in ϵ and Δ plane. Here, the first thing to notice is the absence of HSS solutions. Thus, even a small heterogeneity may remove the HSS solutions. To understand more about this, we have calculated the stable steady-state solutions for the two cases, namely, $\Delta = 0$ and $\Delta \neq 0$, numerically. It is found that the HSS solution branch which is stable for $\Delta = 0$ splits into two branches, as

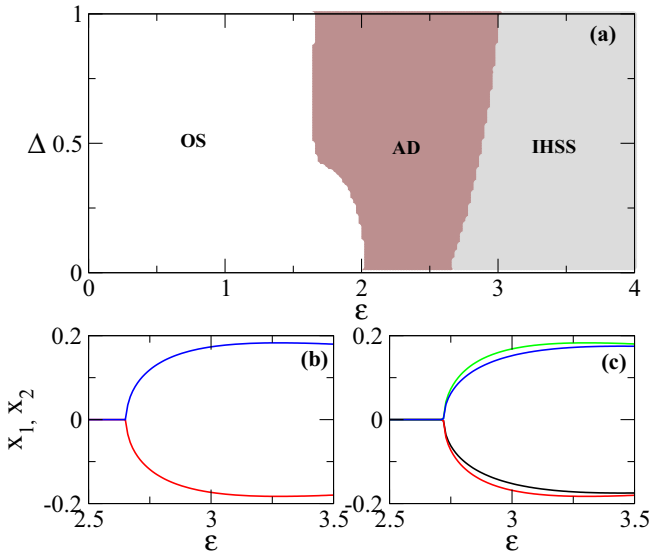

FIG. 4. (Color online) (a) Different dynamical regions plotted by different colors in $\epsilon - \Delta$ plane for $\gamma = 3$ and $\omega_2 = 2$. The stable steady-state solutions against ϵ are calculated numerically for (b) $\Delta = 0$ and (c) $\Delta = 0.1$. The blue (gray) line in panel (b) denotes one of the HSS solution branches splits into two solution branches due to parameter mismatch as shown by blue and green (gray) lines in panel (c). Similarly, the other HSS solution branch also splits into two branches.

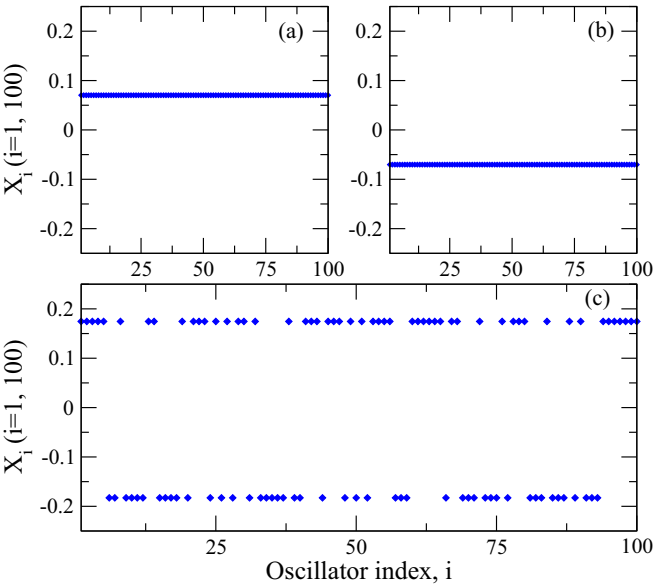

FIG. 5. (Color online) A representative one-state cluster in (a) and (b), and a two-state cluster in (c) for a network of $N = 100$ indirectly coupled identical SL oscillators. In all three diagrams the initial conditions for all oscillators are different, but the parameter values of the system are fixed to $\gamma = 2.5$,$\epsilon = 8.5$, and $\omega = 2$.

displayed in Figs. 4(b) and 4(c). Now, the two mismatched oscillators occupy these new steady states for a particular initial condition. This explains the absence of HSS solution in the parameter mismatch case. This result holds true even for a small amount of mismatch. This is quite different from the results reported for mean-field diffusion coupling [23], where the HSS solution branches become unstable due to parameter mismatch.

At last, we consider the oscillation quenching states for the case where $N > 2$ identical SL oscillators are coupled indirectly via environment. We have found a similar route to oscillation quenching for this system (results not reported). Here, the steady states of N oscillators crucially depend on the initial conditions. For the quenched oscillation regime in the parameter space, there can be either one or two stable steady states for all oscillators. So, all oscillators can form either a one-state HSS cluster shown in Figs. 5(a) and 5(b) or a stable two-state IHSS cluster shown in Fig. 5(c) for the same value of the parameters ϵ and γ.

IV. CONCLUSION

In summary, we have studied a system of limit cycle oscillators coupled indirectly via dynamic environment in the absence of direct interaction among the oscillators. The regions of various dynamical regimes are obtained numerically, which are further well corroborated analytically in the parameter space of coupling strength and decay parameter of the environment. We uncover that the route from oscillatory solutions to quenching of oscillation crucially depends on the decay parameter of the environment. For sufficiently larger decay rate of the medium, γ, the system first stabilizes to trivial fixed point, namely, the origin, followed by the stabilization of HSS and IHSS through pitchfork bifurcations, as the value of coupling strength is increased. However, for a smaller value of decay rate of the environment, HSS solutions are stabilized by Hopf bifurcation. Also, the coexisting region of stable IHSS solutions with HSS solutions appears to decrease for lower values of γ. The interesting thing to note here is the behavior of dynamical regime, where oscillatory solution coexist with quenched oscillation state. In all the previous studies [12,19,23], it is observed that in this bistable dynamical regime the oscillatory solution are in phase while for the quenched oscillation state IHSS solutions are obtained. However, in this particular coupling scheme, we have observed that the antiphase oscillatory solution coexists with HSS solutions. It is also found that each HSS solution branch splits into two by introducing a small parameter mismatch leading to inhomogeneity for this system. Extension of our findings for a network of identical indirectly coupled SL oscillators leads to the fact that the transition from one state to other is preserved under this coupling scheme. As we have studied a generic model of indirectly coupled self-sustained oscillators, our results can be applied to a wide class of systems ranging from biological networks to laser models where the interaction among elements is via common environment. This study can be further extended to indirectly coupled chaotic oscillators [48] and we believe that these studies will improve our understanding of various indirectly coupled biological and chemical systems. Now, there are experimental observations related to oscillation suppression in the populations of BZ catalytic particles [30] as well as in synthetically engineered bacteria [49], and we thus hope our studies can provide a mechanism for oscillation quenching in such systems where the elements

interact via a common environment in the absence of direct coupling.

ACKNOWLEDGMENT

We thank the Department of Science and Technology (DST), Government of India, for financial support.

[1] A. Pikovsky, M. Rosenblum, and J. Kurths, *Synchronization: A Universal Concept in Nonlinear Sciences* (Cambridge University Press, Cambridge, 2003).
[2] S. Boccaletti, J. Kurths, G. Osipov, D. L. Valladares, and C. Zhou, Phys. Rep. **366**, 1 (2002).
[3] M. Laskhmanan and D. V. Senthilkumar, *Dynamics of Nonlinear Time Delay Systems* (Springer, Berlin, 2010).
[4] G. Saxena, A. Prasad, and R. Ramaswamy, Phys. Rep. **521**, 205 (2012).
[5] A. Koseska, E. Volkov, and J. Kurths, Phys. Rep. **531**, 173 (2013).
[6] B. Gallego and P. Cesso, J. Climate **14**, 2815 (2001).
[7] Y. Zhai, I. Z. Kiss, and J. L. Hudson, Phys. Rev. E **69**, 026208 (2004).
[8] P. Kumar, A. Prasad, and R. Ghosh, J. Phys. B **41**, 135402 (2008).
[9] G. B. Ermentrout and N. Kopel, SIAM J. Appl. Math. **50**, 125 (1990).
[10] M. F. Crowley and I. R. Epstein, J. Phys. Chem. **93**, 2496 (1989).
[11] M. Toiya, V. K. Vanag, and I. R. Epstein, Angew. Chem. Int. Ed. **47**, 7753 (2008).
[12] M. Dolnik and M. Marek, J. Phys. Chem. **92**, 2452 (1988).
[13] K. P. Zeyer, M. Mangold, and E. D. Gilles, J. Phys. Chem. A **105**, 7216 (2001).
[14] M. Heinrich, T. Dahms, V. Flunkert, S. W. Teitsworth, and E. Schöll, New. J. Phys. **12**, 113030 (2010).
[15] R. Curtu, Phys. D **239**, 504 (2010).
[16] A. Koseska, E. Volkov, and J. Kurths, Chaos **20**, 023132 (2010).
[17] K. Tsaneva-Atanasova, C. L. Zimliki, R. Bertram, and A. Sherman, Biophys. J. **90**, 3434 (2006).
[18] N. Suzuki, S. Furusawa, and K. Kaneko, PloS ONE **6**, e27232 (2011).
[19] W. Zou, D. V. Senthilkumar, A. Koseska, and J. Kurths, Phys. Rev. E **88**, 050901(R) (2013).
[20] A. Zakharova, I. Schneider, Y. N. Kyrychko, K. B. Blyuss, A. Koseska, B. Fiedler, and E. Schöll, Euro. Phys. Lett. **104**, 50004 (2013).
[21] A. Sharma and M. D. Shrimali, Phys. Rev. E **85**, 057204 (2012).
[22] A. Sharma, K. Suresh, K. Thamilmaran, A. Prasad, and M. D. Shrimali, Nonlinear Dyn. **76**, 1797 (2014).
[23] T. Banerjee and D. Ghosh, Phys. Rev. E **89**, 052912 (2014).
[24] T. Banerjee and D. Ghosh, Phys. Rev. E **89**, 062902 (2014).
[25] N. K. Kamal, P. R. Sharma, and M. D. Shrimali, Pramana J. Phys. **84**, 237 (2015).
[26] C. R. Hens, O. I. Olusola, P. Pal, and S. K. Dana, Phys. Rev. E **88**, 034902 (2013).
[27] A. Sharma, P. R. Sharma, and M. D. Shrimali, Phys. Lett. A **376**, 1562 (2012).
[28] D. Ghosh and T. Banerjee, Phys. Rev. E **90**, 062908 (2014).
[29] J. Garcia-Ojalvo, M. B. Elowitz, and S. H. Strogatz, Proc. Natl. Acad. Sci. USA **101**, 10955 (2004).
[30] A. F. Taylor, M. R. Tinsley, F. Wang, Z. Huang, and K. Showalter, Science **323**, 614 (2009).
[31] J. Zamora-Munt, C. Masoller, J. Garcia-Ojalvo, and R. Roy, Phys. Rev. Lett. **105**, 264101 (2010).
[32] T. Gregor, K. Fujimoto, N. Masaki, and S. Sawai, Science **328**, 1021 (2010).
[33] W. Y. Chiang, Y. X. Li, and P. Y. Lai, Phys. Rev. E **84**, 041921 (2011).
[34] V. Resmi, G. Ambika, and R. E. Amritkar, Phys. Rev. E **81**, 046216 (2010).
[35] V. Resmi, G. Ambika, R. E. Amritkar, and G. Rangarajan, Phys. Rev. E **85**, 046211 (2012).
[36] V. Resmi, G. Ambika, and R. E. Amritkar, Phys. Rev. E **84**, 046212 (2011).
[37] R. Toth, A. F. Taylor, and M. R. Tinsley, J. Phys. Chem. B **110**, 10170 (2006).
[38] A. Kuznetsov, M. Kærn, and N. Kopell, SIAM J. Appl. Math. **65**, 392 (2004).
[39] J. Javaloyes, M. Perrin, and A. Politi, Phys. Rev. E **78**, 011108 (2008).
[40] A. Camilli and B. L. Bassler, Science **311**, 1113 (2006).
[41] S. De Monte, F. d'Ovidio, S. Danø, and P. G. Sørensen, Proc. Natl. Acad. Sci. USA **104**, 18377 (2007).
[42] D. Gonze, S. Bernard, C. Waltermann, A. Kramer, and H. Herzel, Biophys. J. **89**, 120 (2005).
[43] B.-W. Li, C. Fu, H. Zhang, and X. Wang, Phys. Rev. E **86**, 046207 (2012).
[44] D. J. Schwab, A. Baetica, and P. Mehta, Phys. D (Amsterdam, Neth.) **241**, 1782 (2012).
[45] B. Ermentrout, *Simulating, Analyzing, and Animating Dynamical Systems: A Guide to Xppaut for Researchers and Students (Software, Environments, Tools)* (SIAM Press, Philadelphia, 2002).
[46] J. Guckenheimer and P. Holmes, *Nonlinear Oscillations, Dynamical Systems, and Bifurcations of Vector Fields*, Applied Mathematical Sciences Vol. 42 (Springer-Verlag, Berlin, 1983).
[47] K. T. Alligood, T. D. Sauer, and J. A. Yorke, *CHAOS: An Introduction to Dynamical Systems* (Springer-Verlag, Berlin, 1996).
[48] Kamal *et al.* (unpublished).
[49] T. Danino, O. Mondragón-Palomino, L. Tsimring, and J. Hasty, Nature (London) **463**, 326 (2010).